Asymmetrical Contributions of Subunit Pore Regions to Ion Selectivity in an Inward Rectifier K⁺ Channel

Scott K. Silverman,* Henry A. Lester,# and Dennis A. Dougherty*

*Division of Chemistry and Chemical Engineering, and #Division of Biology, California Institute of Technology, Pasadena, California 91125 USA

ABSTRACT   We have investigated aspects of ion selectivity in K⁺ channels by functional expression of wild-type and mutant heteromultimeric G protein-coupled inward-rectifier K⁺ (GIRK) channels in *Xenopus* oocytes. Within the K⁺ channel pore (P) region signature sequence, a large number of point mutations in GIRK1 and GIRK4 subunits have been made at a key tyrosine residue—the "signature" tyrosine of the GYG. Studies of mutant GIRK1/GIRK4 heteromultimers reveal that the GIRK1 and GIRK4 subunits contribute asymmetrically to K⁺ selectivity. The signature tyrosine of GIRK1 can be mutated to many different residues while retaining selectivity; in contrast, the analogous position in GIRK4 must be tyrosine for maximum selectivity. Other residues of the P region also contribute to selectivity, and studies with GIRK1/GIRK4 chimeras reveal that an intact, heteromultimeric P region is necessary and sufficient for optimal K⁺ selectivity. We propose that the GIRK1 and GIRK4 P regions play roles similar to the two P regions of an emerging family of K⁺ channels whose subunits each have two P regions connected in tandem. We find different consequences between similar mutations in inward-rectifier and voltage-gated K⁺ channels, which suggests that the pore structures and selectivity mechanisms in the two classes of channel may not be identical. We confirm that GIRK4 subunits alone can form functional channels in oocytes, but we find that these channels are measurably permeable to Na⁺ and Ca²⁺.

INTRODUCTION

Potassium channels discriminate between Na^+ and K^+ with high selectivity (Hille, 1992). Sequence alignments among K^+ channel subunits (Fig. 1) reveal a conserved pore (P) region "signature sequence" (Heginbotham et al., 1994). Within this signature sequence is the highly conserved GYG triplet, which is critical for ion selectivity (Heginbotham et al., 1992, 1994). Previous work indicates that neither G can be modified without seriously compromising selectivity. Here we focus on the Y, which we shall refer to as the signature tyrosine. We note that in a small fraction of K^+ channels sequenced to date, this Y is an F.

Our strategy for investigating the selectivity role of the P region residues involves functional expression in *Xenopus* oocytes of K^+ channels incorporating wild-type and/or mutated subunits. We have focused on the heteromultimeric G protein-coupled inward-rectifier K^+ (GIRK) channel formed upon coexpression (Krapivinsky et al., 1995a) of the subunits GIRK1 (Kubo et al., 1993b; Dascal et al., 1993) and GIRK4 (Krapivinsky et al., 1995b; Ashford et al., 1994). Previous experiments have shown that the functional GIRK channel is a tetramer and prefers two of each kind of subunit (Silverman et al., 1996b; Tucker et al., 1996; Corey et al., 1998). Note that heteromultimerization is not universal in K^+ channels, as both

voltage-gated (K_v, e.g., Shaker) and inward rectifier (K_{ir}, e.g., ROMK1 and IRK1) homotetramers are known (Miller, 1991; Ho et al., 1993; Tinker et al., 1996; Kubo et al., 1993a).

Our mutagenesis results clearly demonstrate that GIRK1 and GIRK4 contribute asymmetrically to the K^+ selectivity of the functional heteromultimeric channel. Furthermore, by examining GIRK1/GIRK4 chimeras, we show that the heteromultimeric P region is necessary and sufficient for high K^+ selectivity (Krapivinsky et al., 1995a,b; Duprat et al., 1995; Iizuka et al., 1995). We also find that homomultimeric GIRK4 channels are easily and reproducibly observable by the two-electrode voltage clamp technique under typical oocyte expression conditions, and that these channels are permeable to both Na^+ and Ca^{2+}. Robust responses are seen only when the G protein subunits $G_{\beta\gamma}$ are coexpressed; previous work (Krapivinsky et al., 1995a,b; Duprat et al., 1995; Iizuka et al., 1995; Velimirovic et al., 1996; Wischmeyer et al., 1997) had found at best minimal currents from the expression of GIRK4 alone. Finally, our data reveal a striking difference between the consequences of similar mutations in K_{ir} versus K_v channels.

METHODS

DNA clones

GIRK1 (KGA) was available from a previous study (Dascal et al., 1993). GIRK4 was obtained from J. Adelman (Ashford et al., 1994). The m2 acetylcholine receptor (m2AChR) was obtained from E. Peralta and was in the pGEM3Z vector (Lechleiter et al., 1990). The G protein subunits (Gautam et al., 1989; Fong et al., 1986) were available from a previous study (Doupnik et al., 1995). All GIRK constructs and G protein subunits were subcloned into the pMXT vector, obtained from L. Salkoff (Wei et al., 1994). This vector is pBluescript KSII+ (Stratagene) with *Xenopus* β-globin 5'- and 3'-untranslated regions on appropriate ends of the
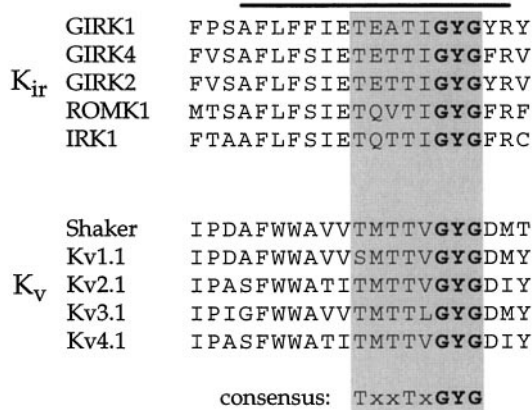

FIGURE 1   Alignment of partial K$^+$ channel sequences reveals a conserved eight-residue pore (P) region signature sequence (*lightly shaded*). The upper bar indicates the nominal extent of the full P region, and the GYG is highlighted. Sequences of both inward-rectifier (K$_{ir}$) and voltage-gated (K$_v$) K$^+$ channels are shown.

polylinker, to enhance expression in oocytes. The m2AChR was linearized with *Hin*dIII, and mRNA was transcribed using the T7 polymerase mMessage mMachine kit from Ambion (Austin, TX). All GIRK4 constructs were linearized with *Sal*I, and mRNA was transcribed using the T3 polymerase mMessage mMachine kit. mRNA concentration was estimated by both UV absorption (A_{260}) and intensity on ethidium bromide-stained agarose gel.

Site-directed mutagenesis

Mutants were created in two ways. In the first method, a two-step polymerase chain reaction (PCR) procedure was employed as follows: two complementary oligonucleotides incorporating the desired point mutations (forward and reverse mutagenic oligos) were synthesized and paired with appropriate outer primers in a first round of PCR (two separate reactions), using *Pfu* polymerase (Stratagene), Expand (Boehringer), or *Pwo* polymerase (Boehringer). The PCR products were purified on agarose gel, then combined with each other and the two outer primers from the first round of PCR, and a second round of PCR was performed. The second PCR product was gel-purified and trimmed on each end with an appropriate restriction enzyme. This product was gel-purified and ligated into the parent construct, previously digested with the same two restriction enzymes and dephosphorylated.

The second method was used when it was clear that many separate mutations were desired in a small region of a protein, or when many (>5) nucleotide changes were the target at the same time. Two restriction sites were introduced (by the PCR cassette method described above) into the plasmid of interest, flanking the region where mutations were desired. Two oligonucleotides were then prepared, such that annealing and insertion of these into the plasmid (previously digested with the two restriction enzymes) provided the desired mutant.

In all cases, mutations were confirmed by automated sequencing of the entire newly synthesized region. Sequences were checked past the two ligation sites. Multimeric GIRK constructs were obtained by methods previously described (Silverman et al., 1996b).

Oocyte preparation and injection

Oocytes were removed from *Xenopus laevis* as described (Quick and Lester, 1994) and maintained at 18°C in ND96 solution with 5% horse serum, changed twice daily. The ND96 solution consisted of (mM) 96 NaCl, 2 KCl, 1 MgCl$_2$, 1.8 CaCl$_2$, 5 HEPES, supplemented with 2.5 mM sodium pyruvate, 50 μg/ml gentamicin, and 0.6 mM theophylline, at pH 7.5 (NaOH). Oocytes were injected with 50 nl of water solution containing 0.05–12.5 ng of GIRK mRNA. Where indicated, oocytes were coinjected

with other samples as follows: 3 ng of m2AChR mRNA; 5 ng of mRNA encoding each G protein subunit G$_{\beta 1}$ and G$_{\gamma 2}$ (collectively G$_{\beta\gamma}$); and 12.5 ng of fully phosphorothioated XIR antisense oligonucleotide KHA2 (5'-CTGAGGACTTGGTGCCATTCT-3') (Hedin et al., 1996), prepared at the Biopolymer Synthesis facility of the Beckman Institute at Caltech.

Electrophysiology

Two-electrode voltage clamp recordings were performed 1–6 days postinjection at room temperature ($\sim$20°C), using a GeneClamp 500 amplifier and pCLAMP software (Axon Instruments, Foster City, CA). Microelectrodes were filled with 3 M KCl and had resistances of 0.5–2 MΩ. Oocytes were continuously perfused with a nominally calcium-free bath solution of 98 mM monovalent cation, 1 mM MgCl$_2$, and 5 mM HEPES (pH 7.5). The monovalent cations were provided as NaCl, KCl, CsCl, or *N*-methyl-D-glucamine (NMDG); the pH was adjusted with NaOH, KOH, NMDG, or HCl, respectively. Other compounds were added to the recording solution from concentrated aqueous stocks immediately before recording. Acetylcholine (ACh) was added to 1 μM from a 1 M stock. Cs$^+$ was added to 1 mM from a 1 M CsCl stock (for Cs$^+$ block of K$^+$ currents). Ca^{2+} was added to 5 mM from a 1 M CaCl$_2$ stock.

K$^+$ currents were quantified at a membrane holding potential of -80 mV in response to either 98 mM extracellular K$^+$ with 1 μM ACh ($I_{K,ACh}$, when m2AChR was coexpressed) or to 98 mM extracellular K$^+$ alone (I_K). Ionic conductance ratios were determined as ratios of currents at 98 mM test ion. Permeability ratios were determined from reversal potential measurements at 98 mM test ion (Hille, 1992; Heginbotham et al., 1994). Currents are reported as mean $\pm$ SEM (number of oocytes). In all figures showing current traces, the labeled bars indicate bath application of 98 mM Na$^+$, K$^+$, or Cs$^+$; 5 mM Ca^{2+}; and 1 μM ACh. Where no bar is shown, the bath solution contained 98 mM NMDG as the only monovalent cation. A complete description of all experiments, including those for which data are referred to but not shown, may be found in Silverman (1998). To quantify ion selectivities, we use two selectivity measures: 1) the ionic conductance ratio I_{Na}/I_K, and 2) the permeability ratio P_{Na}/P_K (similar notation is used for comparison between any two ions). Both measures are valid representations of a channel's ion selectivity (Hille, 1992).

RESULTS

The GIRK channel under consideration comprises two different kinds of subunit, GIRK1 (**1**) and GIRK4 (**4**). Wild-type heteromultimeric **1**/**4** channels prefer a stoichiometry of 2:2 GIRK1:GIRK4 and are highly selective for K$^+$ over Na$^+$. As described in more detail below, we have evidence that some GIRK subunits can assemble with nonstandard stoichiometries. To control the stoichiometry, we studied GIRK1-GIRK4 dimeric constructs, which we symbolize as **1**-**4** (Silverman et al., 1996b). We and others have used such multimeric channels to constrain the subunit stoichiometry of functional K$^+$ channels (Silverman et al., 1996b, and references therein). A representative current trace from an oocyte expressing the wild-type **1**-**4** dimer is shown in Fig. 2. The **1**-**4** dimer is indistinguishable from the "wild-type" channel obtained by expressing separately **1** and **4** (symbolized as **1** + **4**). Even when the **1**-**4** K$^+$ currents were very large, very little if any Na$^+$ current was observed (Table 1).

Expression of GYG mutants in dimeric GIRK1-GIRK4 constructs reveals pore asymmetry

We have studied a large number of **1**-**4** dimers with mutations at the signature tyrosine, to determine the effects on
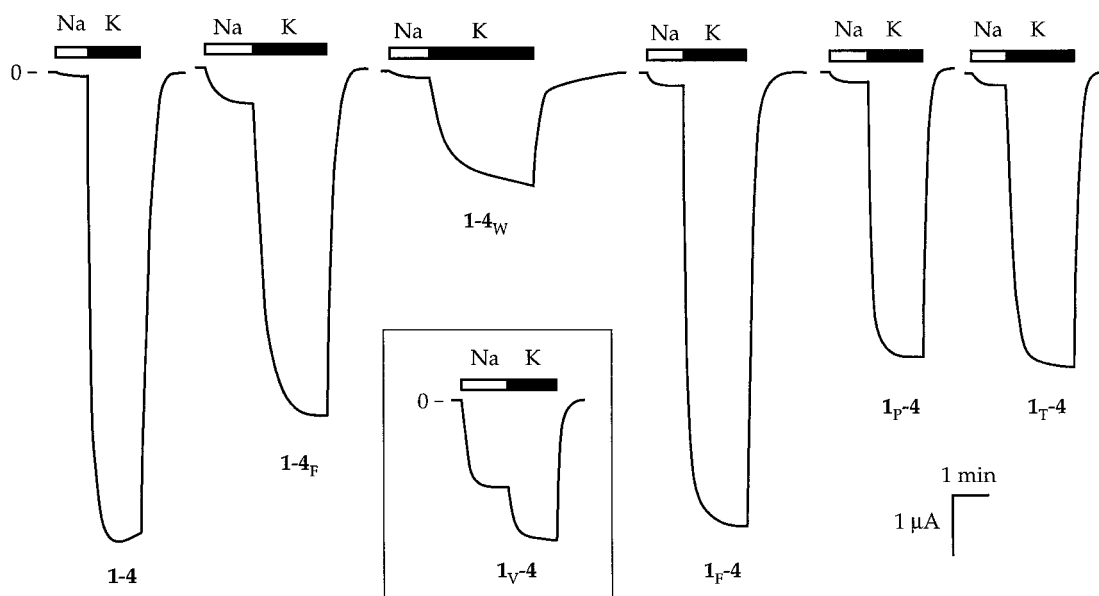
FIGURE 2   Representative current traces from oocytes injected with mRNA for wild-type **1**-**4** dimer and various signature tyrosine mutants of **1**-**4**. Recordings for **1**-**4** were performed 53 h after injection of 0.5 ng mRNA. Recordings for **1**-**4**$_F$ and **1**-**4**$_W$ were performed 84–95 h after injection of 6.25 ng mRNA (+ $G_{\beta\gamma}$ for **1**-**4**$_W$). Recordings for all **1**$_X$-**4** mutants were performed 80–95 h after injection of 6.25–12.5 ng mRNA + $G_{\beta\gamma}$. Another trace for the **1**$_V$-**4** mutant (*boxed*) is shown in Fig. 3.

ion selectivity. Signature tyrosine mutations are designated by subscripts; for example, **1**-**4**$_F$ has the GYG $\rightarrow$ GFG mutation in the GIRK4 subunit only. In the **1**-**4** dimer, the most conservative possible mutation of the GIRK4 signature tyrosine, **1**-**4**$_F$, led to a measurable loss of K^+ selectivity (Table 1). Although the Na^+ permeability of **1**-**4**$_F$ was

evident (Fig. 2), K^+ currents through the channel remained blocked in a voltage-dependent manner by 1 mM Cs^+ as for wild-type **1**-**4** (data not shown), showing that the mutant channel's integrity was not substantially compromised. We made several other mutations at the GIRK4 signature tyrosine. Expression of **1**-**4**$_W$ led to moderate currents above

TABLE 1   Conductance and permeability ratios for GIRK channels

	1–4 channels			**4** channels		
mRNA	I_{Na}/I_K	P_{Na}/P_K	mRNA	I_{Na}/I_K	P_{Na}/P_K	P_{Cs}/P_K
1–4	0.014 ± 0.001		**1 + 4**	<0.02		
1–4$_F$	0.10 ± 0.01	0.55 ± 0.03	(wild type)			
1–4$_W$	≤ 0.1					
1$_F$–**4**	0.026 ± 0.001		**4**	up to 0.4	0.11–0.27	
1$_P$–**4**	0.053 ± 0.005		**4**$_F$	0.11 ± 0.01	0.25 ± 0.02	
1$_T$–**4**	0.036 ± 0.003		**4**$_W$	~ 0.25	0.34 ± 0.02	
1$_A$–**4**	≤ 0.2		**4**$_V$	0.74 ± 0.01	0.79 ± 0.02	0.91 ± 0.02
1$_C$–**4**	≤ 0.2		**4**$_L$	0.74 ± 0.01	0.72 ± 0.02	0.91 ± 0.04
1$_D$–**4**	≤ 0.2		**4**$_A$	—	0.77 ± 0.05	
1$_G$–**4**	0.10 ± 0.01		**4**$_C$	—	0.79 ± 0.05	
1$_I$–**4**	≤ 0.2		**4**$_S$	1.41 ± 0.06	0.62 ± 0.01	
1$_L$–**4**	≤ 0.2		**1 + 4**$_V$		0.81 ± 0.02	0.92 ± 0.03
1$_M$–**4**	≤ 0.2		**4 + 4**$_V$		0.78 ± 0.02	0.88 ± 0.04
1$_N$–**4**	$\geq 0.30 \pm 0.02$		**4–4**	up to 0.3	0.53 ± 0.03	
1$_Q$–**4**	≤ 0.2		**4–4**$_V$	—	0.79 ± 0.02	
1$_R$–**4**	$\geq 0.33 \pm 0.02$		**4(1)**	0.45 ± 0.01	0.64 ± 0.02	
1$_S$–**4**	≤ 0.2		**4(1)–4(1)**	0.47 ± 0.02	0.60 ± 0.02	0.71 ± 0.04
1$_W$–**4**	≤ 0.2		**4(1)–4**$_V$	—	0.63 ± 0.02	
1$_V$–**4**	0.64 ± 0.01	0.76 ± 0.02				

Each data value is derived from at least three independent measurements. Blank spaces indicate data are not collected. —, Poorly defined because of desensitization or slow activation (data not shown). Oocytes were injected with mRNA and recordings were performed as described in the figure legends. For the monomer + **4**$_V$ coinjections, oocytes were coinjected with 1.25 ng wild-type **1** or **4** mRNA. For **4(1)**, oocytes were injected with 6.25 ng mRNA. For some of the channels, the conductance and permeability ratios are lower or upper limits as indicated, because the K^+-selective oocyte background could not be subtracted from the small observed signals.

background (Fig. 2), but the conductance ratio I_{Na}/I_K could not be determined more precisely than ≤ 0.1. The $\mathbf{1}$-$\mathbf{4}_C$ and $\mathbf{1}$-$\mathbf{4}_V$ mutants failed to give signals above background (data not shown).

In sharp contrast, the signature tyrosine of GIRK1 is quite tolerant to substitution. The dimer $\mathbf{1}_F$-$\mathbf{4}$ gave large currents with only slight Na$^+$ permeability (Fig. 2); these currents were blocked by 1 mM Cs$^+$ (data not shown). Surprisingly, the proline mutant $\mathbf{1}_P$-$\mathbf{4}$ and the threonine mutant $\mathbf{1}_T$-$\mathbf{4}$ also gave large, K$^+$-selective signals (Fig. 2); K$^+$ currents through the $\mathbf{1}_P$-$\mathbf{4}$ channel were blocked by 1 mM Cs$^+$ (data not shown; $\mathbf{1}_T$-$\mathbf{4}$ was not tested). The collective results with GIRK1 and GIRK4 GYG mutants demonstrate that the GIRK1 and GIRK4 subunits contribute asymmetrically to ion selectivity.

Because the GIRK1 signature tyrosine seemed to be quite tolerant of substitution, we examined most of the other natural amino acids at this position. Substitution of the $\mathbf{1}$-$\mathbf{4}$ GIRK1 signature tyrosine with any of A, C, D, G, I, L, M, Q, S, or W gave moderate 1–2-μA signals with at least moderate K$^+$ selectivity (Table 1). Substitution of Y with N or R in $\mathbf{1}_N$-$\mathbf{4}$ or $\mathbf{1}_R$-$\mathbf{4}$ led to very weak signals (≤ 1 μA), but the Na$^+$ permeability was clearly greater than that of wild-type $\mathbf{1}$-$\mathbf{4}$. Of all of the amino acids tested, only valine gave large signals with essentially no selectivity for K$^+$ over Na$^+$ when incorporated into the GIRK1 subunit of $\mathbf{1}$-$\mathbf{4}$ (Fig. 3 A). The $\mathbf{1}_V$-$\mathbf{4}$ channel was also permeable to Ca^{2+} (Fig. 3 A). Because $\mathbf{1}_V$-$\mathbf{4}$ gave
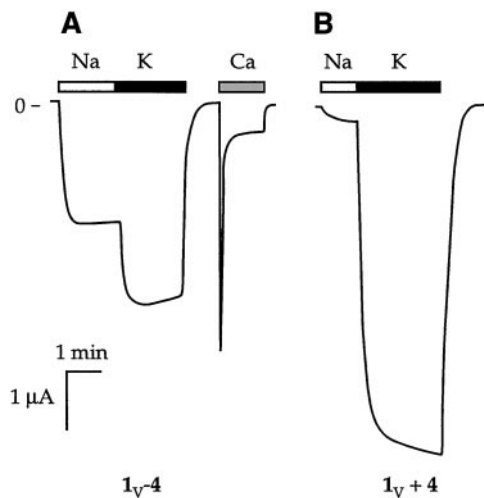
FIGURE 3   Current traces for oocytes expressing the $\mathbf{1}$-$\mathbf{4}$ dimer and $\mathbf{1}_V$ + $\mathbf{4}$ monomers. (A) $\mathbf{1}_V$-$\mathbf{4}$. (B) $\mathbf{1}_V$ + $\mathbf{4}$. Recordings were performed (A) 95 h or (B) 42 h after injection of (A) 6.25 ng $\mathbf{1}_V$-$\mathbf{4}$ mRNA or (B) 1.25 ng each $\mathbf{1}_V$ + $\mathbf{4}$ mRNA + G$_{\beta\gamma}$. The absolute magnitude of the $\mathbf{1}_V$-$\mathbf{4}$ K$^+$ current varied from oocyte batch to batch. A typical result 85 h after injection of 12.5 ng $\mathbf{1}_V$-$\mathbf{4}$ mRNA + G$_{\beta\gamma}$ was $-I_K$ = 1805 $\pm$ 129 nA (n = 6). Occasionally, even larger currents ($\sim$4 μA) were observed. For the $\mathbf{1}_V$ + $\mathbf{4}$ experiment shown in B, $-I_K$ = 5690 $\pm$ 520 nA (n = 6), and $I_{Na}/I_K \approx$ 0.04. Traces with similarly high K$^+$ selectivity were also observed when the ratio of $\mathbf{1}_V$ to $\mathbf{4}$ mRNA was 5:1 (data not shown). The $\mathbf{1}$ + $\mathbf{4}$ and $\mathbf{1}_V$ + $\mathbf{4}$ mRNA combinations yielded similar current-versus-[K$^+$] profiles when tested at 10, 30, and 98 mM K$^+$ (data not shown), implying that the large K$^+$-selective currents from $\mathbf{1}_V$ + $\mathbf{4}$ are not an artefact of the nonphysiological high K$^+$ concentration during recording.

substantial currents whereas $\mathbf{1}$-$\mathbf{4}_V$ did not, we tested $\mathbf{1}_V$-$\mathbf{4}_V$, which gave no signal (data not shown).

P-region chimeras of GIRK1 and GIRK4 establish that an intact, heteromultimeric P region is necessary and sufficient for high K$^+$ selectivity

The experiments described above examine the roles of the GIRK1 and GIRK4 signature tyrosine residues in ion selectivity. To explore the contributions of other P region residues, we prepared two P-region chimeras, which we term $\mathbf{1(4)}$ and $\mathbf{4(1)}$ (Fig. 4). The subunit in parentheses indicates the origin of the P region, and the subunit outside the parentheses shows the source of all remaining nonpore residues. Thus $\mathbf{1(4)}$ comprises the nonpore residues of $\mathbf{1}$ plus the P region of $\mathbf{4}$. Note that the P regions of $\mathbf{1}$ and $\mathbf{4}$ differ in five residues, so $\mathbf{1(4)}$ and $\mathbf{4(1)}$ may each be described as quintuple mutants. The most informative results came from dimer constructs of these chimeric subunits; qualitatively similar results were obtained by coexpression of chimera monomers (data not shown; see Silverman, 1998, for further details).

We prepared nine dimer combinations of the subunits $\mathbf{1}$, $\mathbf{4}$, $\mathbf{1(4)}$, and $\mathbf{4(1)}$ (Fig. 5). The $\mathbf{1}$-$\mathbf{1}$ dimer was not prepared, as $\mathbf{1}$ alone is known with confidence not to lead to functional channels (Hedin et al., 1996). We prepared the $\mathbf{1}$-$\mathbf{4}$ and $\mathbf{4}$-$\mathbf{1}$ dimers in an earlier study and showed that the subunit connectivity does not strongly affect the channel, as the two constructs gave indistinguishable signals (Silverman et al., 1996b).

Dimers with only GIRK1 nonpore regions (*left column* of Fig. 5) did not give significant currents ($-I_K$ < 700 nA, > 80 h after coinjection with G$_{\beta\gamma}$). Chimera dimers with mixed GIRK1/GIRK4 nonpore regions (*middle column*) did
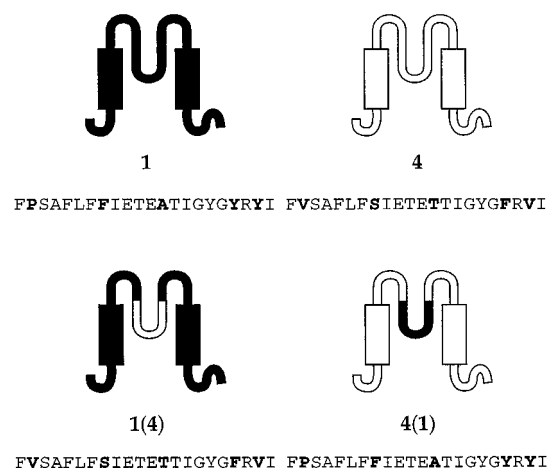

FIGURE 4   Schematic diagrams of the wild-type GIRK subunits $\mathbf{1}$ and $\mathbf{4}$ and of the chimera subunits $\mathbf{1(4)}$ and $\mathbf{4(1)}$. Each subunit's two transmembrane domains are depicted as rectangles, and the P region is the intervening loop. GIRK1 residues are in black, and GIRK4 residues are in white. For clarity, the P regions and N- and C-terminal tails are not depicted to scale. The P-region sequences of each construct are shown (compare Fig. 1); the five P-region residues differing between GIRK1 and GIRK4 are in boldface.
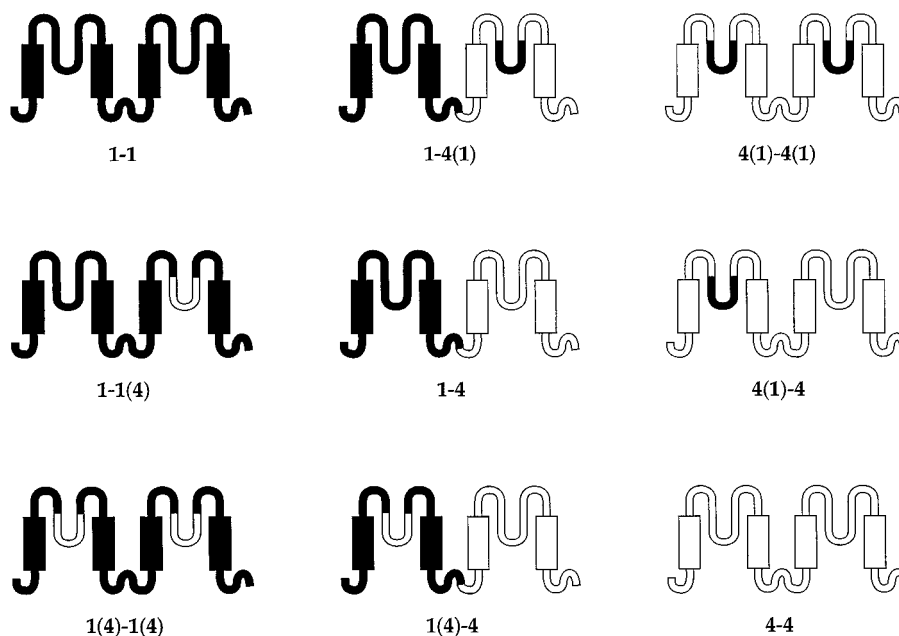
FIGURE 5 The GIRK chimera dimers. All except the **1-1** dimer were prepared. The **1(4)-4(1)** dimer (not pictured) was tested but did not give signals above background. The dimers in the corners are symmetrical, in that switching the subunits gives the same amino acid sequence. The other dimers (and the **1(4)-4(1)** dimer) are asymmetrical. For **1-4** and **4(1)-4**, their switched-subunits counterparts **4-1** and **4-4(1)** were also prepared (see text).

not express well either. In contrast, dimers with nonpore regions from GIRK4 only (*right column* of Fig. 5) provided substantial and informative currents. This suggests that the nonpore regions may contribute more to assembly than to ion selectivity.

In the **4(1)-4** dimer, the residues in the two P regions parallel those of the wild-type **1-4** heteromultimer, but the nonpore regions are taken only from GIRK4. The **4(1)-4** channel showed high K^+ selectivity, comparable to that of wild-type **1-4** (Fig. 6 *A*). The subunit connection order does not matter, as the signals from **4(1)-4** and **4-4(1)** were indistinguishable (Fig. 6 *B*). The voltage-step recordings of **4(1)-4** (Fig. 7) resembled those of wild-type **1-4**. In contrast, the dimers **4-4** and **4(1)-4(1)** were not highly K^+-selective (Fig. 6, *C* and *D*, and Table 1). The **4-4** channel had significant Na^+ permeability but was blocked by 1 mM Cs^+, whereas the **4(1)-4(1)** channel showed little selectivity among Na^+, K^+, and Cs^+. These constructs together establish that a heteromultimeric GIRK1/GIRK4 P region is sufficient to provide essentially wild-type K^+ selectivity, even in the context of nonpore regions taken solely from GIRK4.

Note that the chimera subunits **1(4)** and **4(1)** swap all five of the residues that differ between the P regions of GIRK1 and GIRK4. Previously, one of these five residues (GIRK1 F137/GIRK4 S143) was identified as distinguishing the contributions of GIRK1 and GIRK4 to the heteromultimer (Kofuji et al., 1996; Chan et al., 1996). We therefore created chimera dimers similar to **4(1)-4**, in which one of the two P regions had either zero or five mutations, and the other one or four mutations (see Silverman, 1998, for further details). In contrast to the highly K^+-selective parent dimer **4(1)-4**, all of these more elaborate constructs gave large currents with significant Na^+ permeability ($P_{Na}/P_K \geq 0.47$; data not shown). This establishes that an intact, heteromultimeric

P region is necessary as well as sufficient for high K^+ selectivity.

Nonstandard stoichiometries

Throughout this work we have seen several indications that nonstandard stiochiometries—i.e., other than 2:2 GIRK1: GIRK4—can be viable. Although the biological relevance of such assemblies may be minimal, they do have interesting implications for subunit assembly and even ion selectivity issues. Here we briefly summarize the key observations; a much more detailed analysis is presented elsewhere (Silverman, 1998).

When oocytes were injected with mRNA encoding **4** alone, large K^+ currents were observed 1–6 days later, but only when the G protein subunits $G_{\beta\gamma}$ were coexpressed (Fig. 8 *A*). Note that with wild-type **1** + **4** channels, significant K^+ currents are observed even in the absence of coexpressed $G_{\beta\gamma}$ (Krapivinsky et al., 1995a). Surprisingly, oocytes expressing **4** alone developed significant Na^+ currents that were much larger than those of uninjected oocytes or oocytes expressing **1** + **4** (Fig. 8 and Table 1). The values of P_{Na}/P_K for **4** were somewhat variable (0.11–0.27) but clearly much less than unity. The **4**-only channels were permeable to Ca^{2+}; as in an earlier study (Silverman et al., 1996a), we attribute the Ca^{2+}-induced signals to chloride currents. Although the currents from GIRK4 expression appeared much too large to be explained by coassembly of **4** with the endogenous oocyte K^+ channel subunit XIR, we verified that antisense inhibition of XIR with the phosphorothioated oligonucleotide KHA2 (Hedin et al., 1996) did not diminish the signal (data not shown). This supports the claim that the currents are indeed due to channels composed solely of **4** subunits. Note that qualitatively similar Na^+
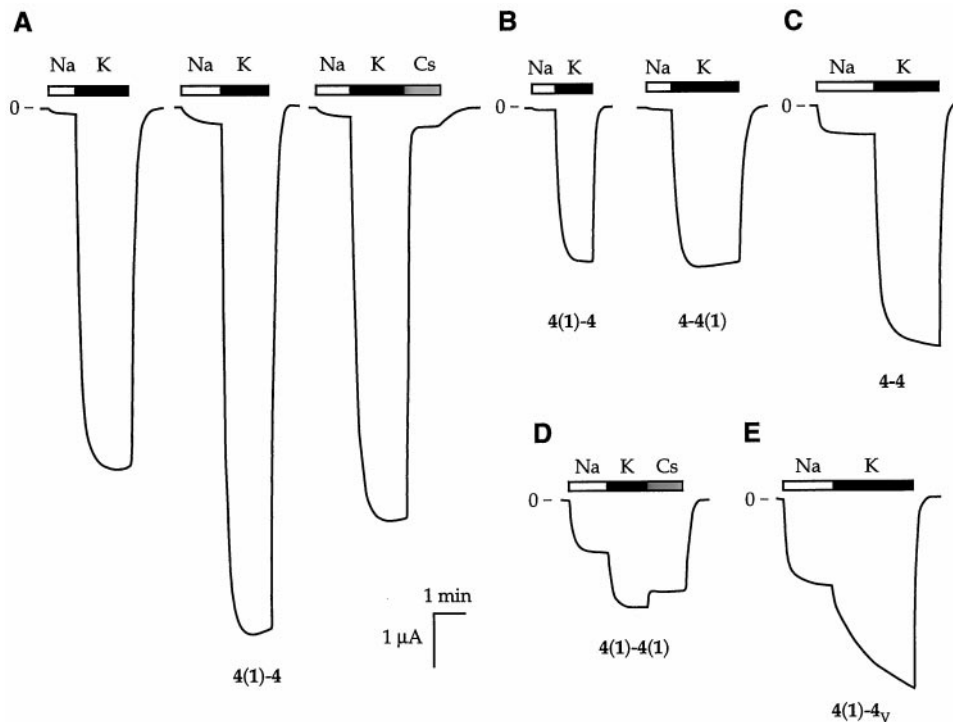
FIGURE 6   Current traces for oocytes injected with **4(1)-4**, **4-4(1)**, **4-4**, **4(1)-4(1)**, or **4(1)-4$_V$** mRNA. (*A*) **4(1)-4**. (*B*) Direct comparison of **4(1)-4** and **4-4(1)**. (*C*) **4-4**. (*D*) **4(1)-4(1)**. (*E*) **4(1)-4$_V$**. For *A*, recordings were performed 40–53 h after injection with 6.25 ng **4(1)-4** mRNA. For *B*, recordings were performed 36 h after injection with 6.25 ng dimer mRNA, and currents ($-I_K$ in nA, n = 6–7) were **4(1)-4**, 3189 $\pm$ 403; **4-4(1)**, 2642 $\pm$ 176. For *C*, recordings were performed 87 h after injection with 12.5 ng **4-4** mRNA + G$_{\beta\gamma}$; typical currents ($-I_K$ in nA, n = 3–9) were as follows: uninjected, 370 $\pm$ 6; **4-4** alone, 427 $\pm$ 40; **4-4** + G$_{\beta\gamma}$, 4156 $\pm$ 64. For *D*, recordings were performed 92 h after injection with 12.5 ng **4(1)-4(1)** mRNA + G$_{\beta\gamma}$. For *E*, recordings were performed 84 h after injection with 6.25 ng **4(1)-4$_V$** mRNA + G$_{\beta\gamma}$. Quantitatively similar results were obtained with **4$_V$-4(1)**, the dimer with the opposite subunit connection order (data not shown). For both **4(1)-4** and **4(1)-4(1)**, G$_{\beta\gamma}$ coexpression was not required to obtain large currents (data not shown); **4(1)-4$_V$** was not tested without G$_{\beta\gamma}$.

permeability was obtained from the **4-4** dimer (Fig. 6 *C*), although the monomer and dimer channels have different current levels, activation time courses, and desensitization.

Although **4**-only channels are only moderately K$^+$-selective, we have investigated the effects of signature tyrosine mutations in such constructs. We find that the conservative
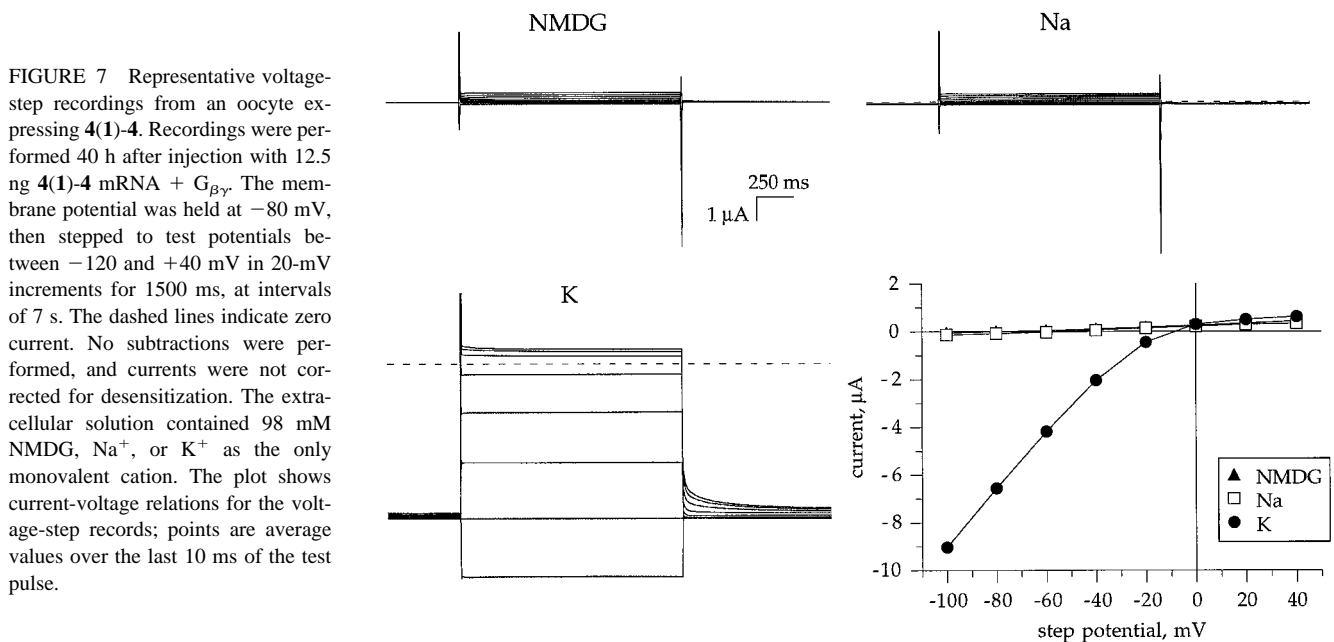
FIGURE 7   Representative voltage-step recordings from an oocyte expressing **4(1)-4**. Recordings were performed 40 h after injection with 12.5 ng **4(1)-4** mRNA + G$_{\beta\gamma}$. The membrane potential was held at −80 mV, then stepped to test potentials between −120 and +40 mV in 20-mV increments for 1500 ms, at intervals of 7 s. The dashed lines indicate zero current. No subtractions were performed, and currents were not corrected for desensitization. The extracellular solution contained 98 mM NMDG, Na$^+$, or K$^+$ as the only monovalent cation. The plot shows current-voltage relations for the voltage-step records; points are average values over the last 10 ms of the test pulse.
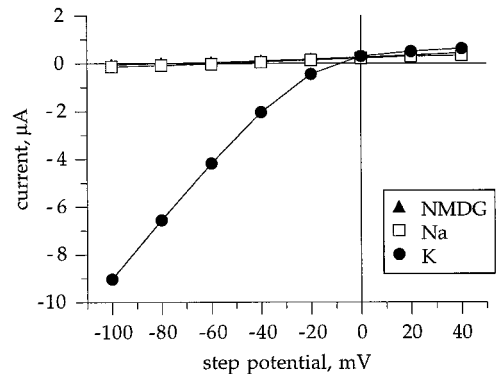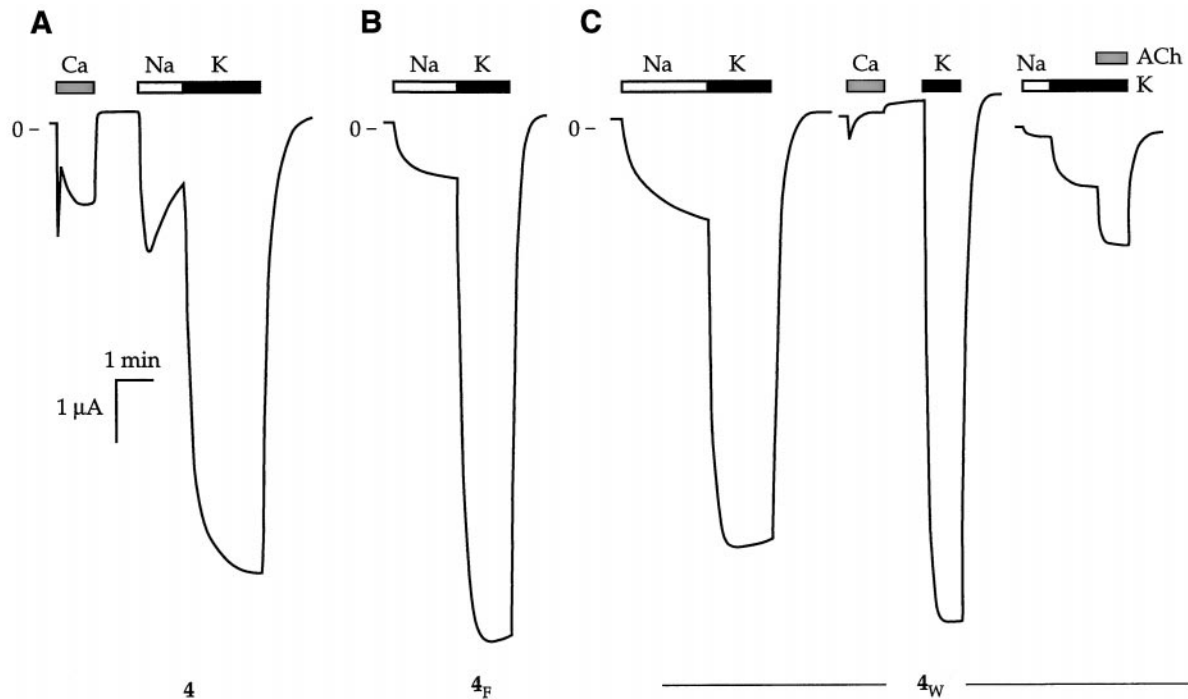
FIGURE 8 Channels from **4**, **4**$_F$, and **4**$_W$ are all permeable to Na$^+$. (*A*) **4**. (*B*) **4**$_F$. (*C*) **4**$_W$. Large currents were observed in all cases only if G$_{\beta\gamma}$ was coexpressed. Traces similar to that in *A* were obtained for **4** oocytes not first exposed to Ca^{2+}. For **4**, 84 h after injection of 12.5 ng **4** mRNA, typical currents ($-I_K$ in nA, $n = 3$–5) were as follows: uninjected, 213 ± 9; **4** alone, 655 ± 34; **4** + G$_{\beta\gamma}$, 11,808 ± 273. The absolute currents from **4**$_F$ and **4**$_W$ were larger than those from wild-type **4**. Typical currents 37 h after injection of 6.25–12.5 ng **4**, **4**$_F$, or **4**$_W$ mRNA + G$_{\beta\gamma}$, currents ($-I_K$ in nA, $n = 3$–7) were as follows: uninjected, 190 ± 15; **4**, 2790 ± 59; **4**$_F$, 4588 ± 178, and **4**$_W$, >10,000.

(i.e., aromatic) mutants **4**$_F$ and **4**$_W$ produce channels with moderate K$^+$ selectivities, comparable to **4**-only channels (Fig. 8 and Table 1). However, the nonconservative mutation **4**$_V$ completely abolished K$^+$ selectivity and conferred Cs$^+$ permeability (Fig. 9; **4** and **4**$_W$ are blocked by Cs$^+$). The **4**$_L$, **4**$_A$, **4**$_C$, and **4**$_S$ subunits were also prepared; when expressed alone, each gave permeability characteristics similar to those of **4**$_V$ (Table 1).

Another indication of nonstandard stoichiometry came from studies of the **1**$_V$-**4** dimeric construct. The results from expression of **1**$_V$-**4** are unambiguous; the resulting channel is nonselective between K$^+$ and Na$^+$ (Fig. 3 *A*). However, coexpression of **1**$_V$ + **4** (i.e., the monomer subunits) gave large signals without significant Na$^+$ conductance (Fig. 3 *B*). We also found an anomalous mRNA dependence for the **1**$_V$ + **4** currents. When the amount of injected **1**$_V$ mRNA was increased fivefold, the resulting currents reproducibly decreased by about the same factor (Table 2). Suspecting a nonstandard subunit stoichiometry in the **1**$_v$ + **4** experiments, we expressed the mutant tetramer **1**$_V$-**4**-**4**-**4** side by side with the previously reported **1**-**4**-**4**-**4** (Silverman et al., 1996b). The **1**$_V$-**4**-**4**-**4** currents were large enough (~2 μA) to be clearly distinguished from nonselective signals such as those from **1**$_V$-**4**, although the conductance ratio could not be determined more precisely than $I_{Na}/I_K \leq 0.1$ (data not shown). Thus it appears that functional 1:3 complexes of GIRK subunits (in particular, 1:3 GIRK1:GIRK4) can form under some circumstances.

Dissimilar consequences of similar mutations in K$_{ir}$ versus K$_v$ channels

In an earlier study, MacKinnon and co-workers reported that the Shaker K$_v$ channel retains at least moderate K$^+$ selectivity when all four GYG tyrosines are mutated to valine (Heginbotham et al., 1994). In contrast, the **4**$_V$ homomultimer reported here is decidedly nonselective between Na$^+$ and K$^+$ (Table 1 and Fig. 9 *A*). Furthermore, the dimeric construct **4**-**4**$_V$ is also nonselective (Table 1 and Fig. 9 *B*). That is, within the context of a **4**-only channel, only two of the four signature tyrosines need be mutated to abolish selectivity. These results highlight a significant difference between the consequences of similar mutations in K$_{ir}$ and K$_v$ channels.

Mutagenesis of the **4**(**1**)-**4** dimer reinforces the view of the GIRK channel as particularly sensitive to GYG mutations. The **4**(**1**)-**4** dimer's high K$^+$ selectivity was lost upon mutating the second signature tyrosine to valine, as in **4**(**1**)-**4**$_V$ (Fig. 6 *E*).

DISCUSSION

Asymmetry in GIRK1/GIRK4 channels

The results with **1**-**4** mutants demonstrate a clear asymmetry in the functional roles of the GIRK1 and GIRK4 subunits. Mutation of the **4** signature tyrosine in the **1**-**4** dimer re-
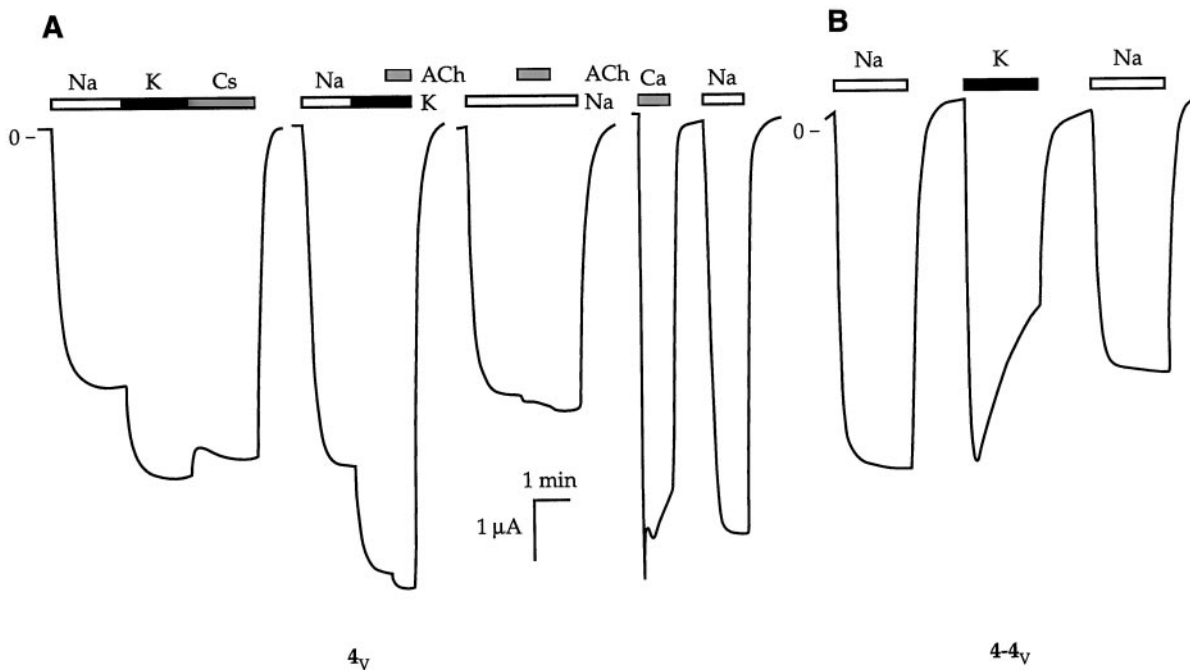
FIGURE 9   GIRK4 channels with a nonconservative Y152V mutation ($\mathbf{4_V}$) are nonselective among Na$^+$, K$^+$, and Cs$^+$; are constitutively activated; and are permeable to Ca^{2+}. (*A*) $\mathbf{4_V}$. (*B*) $\mathbf{4}$-$\mathbf{4_V}$. In *A*, recordings were performed 32–42 h after injection with 6.25 ng $\mathbf{4_V}$ mRNA + m2AChR. In *B*, recordings were performed 99 h after injection of 6.25 ng $\mathbf{4}$-$\mathbf{4_V}$ mRNA.

vealed that this residue is particularly important for K$^+$ selectivity; even mutation to phenylalanine, providing $\mathbf{1}$-$\mathbf{4_F}$, led to a measurably Na$^+$-permeable channel (Fig. 2 and Table 1). Less conservative mutations to $\mathbf{1}$-$\mathbf{4_W}$, $\mathbf{1}$-$\mathbf{4_C}$, or $\mathbf{1}$-$\mathbf{4_V}$ provided channels with much reduced if any current. The $\mathbf{1}$-$\mathbf{4_F}$ channel did not lose all ion selectivity, however, as it remained blocked by Cs$^+$.

In sharp contrast, mutation of the $\mathbf{1}$ signature tyrosine in the $\mathbf{1}$-$\mathbf{4}$ dimer provided in some cases a channel that was approximately as selective as the wild type. In particular, the $\mathbf{1_P}$-$\mathbf{4}$ and $\mathbf{1_T}$-$\mathbf{4}$ dimers gave large enough currents to state with confidence that the resulting channels are highly K$^+$-selective. We conclude that the $\mathbf{1}$ and $\mathbf{4}$ subunits of the GIRK1/GIRK4 heterotetramer make qualitatively different, asymmetrical contributions to the channel's K$^+$ selectivity.

Members of an emerging family of K$^+$ channels contain two P regions per subunit, instead of the conventional single P region (Lesage et al., 1996a,b; Goldstein et al., 1996, 1998; Wei et al., 1996; Ketchum et al., 1995). Typically, only one P region has the conserved GYG triplet, whereas

the other has instead GFG, GLG, or GIG. One system has two GFGs (Ketchum et al., 1995). Nevertheless, channels formed from these subunits are highly K$^+$-selective.

Based on the results reported here, we suggest an analogy between the GIRK1/GIRK4 system and the family of two P domain channels. That is, of the four subunits in the functional $\mathbf{1}$/$\mathbf{4}$ channel, only the two $\mathbf{4}$ subunits must have intact signature tyrosines for normal, high K$^+$ selectivity. In contrast, the $\mathbf{1}$ subunits may have other residues (such as P or T) at this position and be part of a K$^+$-selective channel. In, perhaps, a related observation, Pascual et al. found that mutating two of four signature tyrosines to cysteine in the K$_v$2.1 channel still allows signficant channel activity, whereas four cysteine mutations abolish K$^+$ currents (Pascual et al., 1995). Unfortunately, the Na$^+$/K$^+$ selectivity of their double mutant was not reported. We also note that the K$^+$ channel subunit GIRK2 is highly homologous to GIRK4. The GIRK1/GIRK2 heteromultimeric channel is physiologically relevant, and we surmise that the GIRK1/GIRK2 channel would show the same functional asymmetry as we report here for the GIRK1/GIRK4 heteromultimer.

The experiments with GIRK1/GIRK4 chimeras (Fig. 6) clarify the role of the entire P region in ion selectivity. Expression of the $\mathbf{4(1)}$-$\mathbf{4}$ dimer led to large, highly K$^+$-selective currents. However, the $\mathbf{4(1)}$-$\mathbf{4(1)}$ and $\mathbf{4}$-$\mathbf{4}$ channels both have all four signature tyrosines and yet are decidedly nonselective, a situation that is, to our knowledge, unprecedented. The heteromultimeric P region is finely tuned for K$^+$ selectivity, because the more elaborate chimera dimers involving incomplete P-region swaps are not highly K$^+$-

TABLE 2   **Anomalous 1_V mRNA dependence of 1_V + 4: the current decreases when the amount of 1_V mRNA is increased**

Oocyte batch	$-I_{K,ACh}$ (nA)
Uninjected	53 ± 3 (n = 3)
1_V 1.25 ng + 4	4410 ± 198 (n = 5)
1_V 6.25 ng + 4	1066 ± 185 (n = 5)
1_V 6.25 ng alone	240 ± 26 (n = 4)

Recordings were performed 36 h after injection of the GIRK mRNAs (1.25 ng **4**) + m2AChR.

selective. As a whole, these experiments demonstrate that the intact, heteromultimeric GIRK1/GIRK4 P region is both necessary and sufficient for high K^+ selectivity in these channels.

Comparison of K_{ir} and K_v channels

Our new results with a member of the K_{ir} family stand in sharp contrast to previously reported experiments of Mac-Kinnon and co-workers on the Shaker K_v channel (Heginbotham et al., 1994). The 4_V (K_{ir}) homotetramer reported here is completely nonselective between Na^+ and K^+ (Fig. 9 A), and mutation of just two of four possible GYGs to GVG (using 4-4_V) is enough to obliterate selectivity (Fig. 9 B). The same loss of selectivity is observed upon mutating the highly selective $4(1)$-4—a construct for which the P region is identical to that of the physiologically relevant GIRK1/GIRK4 channel—to $4(1)$-4_V (Fig. 6 E), a change again involving only two of the four signature tyrosines. However, the Shaker (K_v) homotetramer with the quadruple GYG-to-GVG mutation is reported to retain significant K^+ selectivity. Only an upper limit on the selectivity ratio ($P_{Na}/P_K < 0.2$) was determined for this mutant K_v channel, which, although K^+-selective, could be significantly less so than the wild type ($P_{Na}/P_K < 0.02$ by reversal potential measurements, but generally considered to be much more selective). This difference between K_{ir} and K_v channels is striking, because based on sequence similarity, it has been assumed that the two share a common selectivity mechanism. Our data suggest that the pore structures and selectivity mechanisms of K_{ir} and K_v channels may not be identical, although more data would be needed to verify this conclusion.

Variations in subunit stoichiometry

Several observations reported here establish that the canonical 2:2 stoichiometry of hetermeric GIRK channels is not required for formation of a functional channel. We readily observe functional channels upon expression of GIRK4 alone, although coexpression of $G_{\beta\gamma}$ is required. Furthermore, the studies of $1_V + 4$ constructs strongly suggest that a $(1_V)_1(4)_3$ stoichiometry is viable (Fig. 3). Whether such arrangements are biologically relevant remains to be seen, but at the very least our observations highlight the potential pitfalls in studying heteromultimeric systems under heterologous expression conditions.

ADDENDUM

While this paper was under review, the landmark structure determination of the KcsA K^+ channel was reported by MacKinnon and co-workers (Doyle et al., 1998). Our work, like all to follow, must be reevaluated in light of this spectacular result. Briefly, we mention here several key issues. It is clear from observations throughout this work

that there is a substantial preference for aromatic residues (F, Y, W) at the signature tyrosine position. We had earlier interpreted this to be supportive of, but certainly not proof of, the cation-π mechanism of ion selectivity. It is now clear that this is not the case—backbone carbonyl oxygens from the pore region are responsible for selecting K^+ over Na^+.

The central conclusion of this work is that there is asymmetry in the pore region—the GYG units of GIRK1 and GIRK4 contribute unequally to the selectivity filter. The KcsA crystal structure shows fourfold symmetry, although this was imposed on the structure during refinement. Although it is difficult to know with certainty at this point, it seems unlikely that dramatic desymmetrization would occur were this constraint relaxed. This symmetry issue could be related to the other key observation of this work—the significant difference between K_{ir} and K_V channels in response to pore region mutations. Although KcsA is topologically a K_{ir} channel (in that it has only two transmembrane domains), in the pore region it is clearly a K_v channel. The MacKinnon structure raises interesting questions concerning K_V versus K_{ir} channels. In the pore region (Fig. 1), the FWW that is present in all K_V channels is universally replaced by FLF in K_{ir} channels. In the KcsA structure, both members of the WW unit experience crucial contacts with the signature tyrosine that position the selectivity filter, including an explicit W···Y hydrogen bond. These contacts must be substantially altered when FLF replaces FWW, and, in particular, no structure analogous to the W···Y hydrogen bond can be present. Perhaps the different manner that K_{ir} channels have found to position the selectivity filter will account for the differences between K_v and K_{ir} families we have seen. We look forward to further structural data for both classes of K^+ channels.

REFERENCES

Ashford, M. L. J., C. T. Bond, T. A. Blair, and J. P. Adelman. 1994. Cloning and functional expression of a rat heart K_{ATP} channel. *Nature.* 370:456–459.

Chan, K. W., J.-L. Sui, M. Vivaudou, and D. Logothetis. 1996. Control of channel activity through a unique amino acid residue of a G protein-gated inwardly rectifying K^+ channel subunit. *Proc. Natl. Acad. Sci. USA.* 93:14193–14198.

Corey, S., G. Krapivinsky, L. Krapivinsky, and D. E. Clapham. 1998. Number and stoichiometry of subunits in the native atrial G-protein-gated K^+ channel, I_{KACh}. *J. Biol. Chem.* 273:5271–5278.

Dascal, N., W. Schreibmayer, N. F. Lim, W. Wang, C. Chavkin, L. DiMagno, C. Labarca, B. L. Kieffer, C. Gaveriaux-Ruff, D. Trollinger, H. A. Lester, and N. Davidson. 1993. Atrial G protein-activated K^+ channel: expression cloning and molecular properties. *Proc. Natl. Acad. Sci. USA.* 90:10235–10239.

Doupnik, C. A., N. F. Lim, P. Kofuji, N. Davidson, and H. A. Lester. 1995. Intrinsic gating properties of a cloned g-protein-activated inward rectifier K^+ channel. *J. Gen. Physiol.* 106:1–23.

Doyle, D., J. M. Cabral, R. A. Pfuetzner, A. Kuo, J. M. Gulbis, S. L. Cohen, B. T. Chait, and R. MacKinnon. 1998. The structure of the

potassium channel: molecular basis of K$^+$ conduction and selectivity. *Science.* 280:69–77.

Duprat, F., F. Lesage, E. Guillemare, M. Fink, J. P. Hugnot, J. Bigay, M. Lazdunski, G. Romey, and J. Barhanin. 1995. Heterologous multimeric assembly is essential for K$^+$ channel activity of neuronal and cardiac G-protein-activated inward rectifiers. *Biochem. Biophys. Res. Commun.* 212:657–663.

Fong, H. K. W., J. B. Hurley, R. S. Hopkins, R. Miakelye, M. S. Johnson, R. F. Doolittle, and M. I. Simon. 1986. Repetitive segmental structure of the transducin b-subunit—homology with the CDC4 gene and identification of related messenger-RNAs. *Proc. Natl. Acad. Sci. USA.* 83:2162–2166.

Gautam, N., M. Baetcher, R. Aebersold, and M. I. Simon. 1989. A G protein g subunit shares homology with ras proteins. *Science.* 244:917–974.

Goldstein, S. A. N., L. A. Price, D. N. Rosenthal, and M. H. Pausch. 1996. ORK1, a potassium-selective leak channel with two pore domains cloned from *Drosophila melanogaster* by expression in *Saccharomyces cerevisiae. Proc. Natl. Acad. Sci. USA.* 93:13256–13261.

Goldstein, S. A. N., K.-W. Wang, N. Ilan, and M. H. Pausch. 1998. Sequence and function of the two P domain potassium channels: implications of an emerging superfamily. *J. Mol. Med.* 76:13–20.

Hedin, K. E., N. F. Lim, and D. E. Clapham. 1996. Cloning of a *Xenopus laevis* inwardly rectifying K$^+$ channel subunit that permits GIRK1 expression of I$_{KACh}$ currents in oocytes. *Neuron.* 16:423–429.

Heginbotham, L., T. Abramson, and R. MacKinnon. 1992. A functional connection between the pores of distantly related ion channels as revealed by mutant K$^+$ Channels. *Science.* 258:1152–1155.

Heginbotham, L., Z. Lu, T. Abramson, and R. MacKinnon. 1994. Mutations in the K$^+$ channel signature sequence. *Biophys. J.* 66:1061–1067.

Hille, B. 1992. Ionic Channels of Excitable Membranes. Sinauer Associates, Sunderland, MA.

Ho, K., C. G. Nichols, W. J. Lederer, J. Lytton, P. M. Vassiliev, M. V. Kanazirska, and S. C. Hebert. 1993. Cloning and expression of an inwardly rectifying ATP-regulated potassium channel. *Nature.* 362:31–38.

Iizuka, M., Y. Kubo, I. Tsunenari, C. X. Pan, I. Akiba, and T. Kono. 1995. Functional characterization and localization of a cardiac-type inwardly rectifying K$^+$ channel. *Receptors Channels.* 3:299–315.

Ketchum, K. A., W. J. Joiner, A. J. Sellers, L. K. Kaczmarek, and S. A. N. Goldstein. 1995. A new family of outwardly rectifying potassium channel proteins with 2 pore domains in tandem. *Nature.* 376:690–695.

Kofuji, P., C. A. Doupnik, N. Davidson, and H. A. Lester. 1996. A unique P-region residue is required for slow voltage-dependent gating of a G protein-activated inward rectifier K$^+$ channel expressed in *Xenopus* oocytes. *J. Physiol. (Lond.).* 490:633–645.

Krapivinsky, G., E. A. Gordon, K. Wickman, B. Velimirovic, L. Krapivinsky, and D. E. Clapham. 1995a. The G protein-gated atrial K$^+$ channel IK(ACh) is a heteromultimer of 2 inwardly rectifying K$^+$ channel proteins. *Nature.* 374:135–141.

Krapivinsky, G., L. Krapivinsky, B. Velimirovic, K. Wickman, B. Navarro, and D. E. Clapham. 1995b. The cardiac inward rectifier K$^+$ channel subunit, CIR, does not comprise the ATP-sensitive K$^+$ channel, IKATP. *J. Biol. Chem.* 270:28777–28779.

Kubo, Y., T. J. Baldwin, Y. N. Jan, and L. Y. Jan. 1993a. Primary structure and functional expression of a mouse inward rectifier potassium channel. *Nature.* 362:127–133.

Kubo, Y., E. Reuveny, P. A. Slesinger, Y. N. Jan, and L. Y. Jan. 1993b. Primary structure and functional expression of a rat G-protein-coupled muscarinic potassium channel. *Nature.* 364:802–806.

Lechleiter, J., R. Hellmiss, K. Duerson, D. Ennulat, N. David, D. Clapham, and E. Peralta. 1990. Distinct sequence elements control the specificity of G protein activation by muscarinic acetylcholine receptor subtypes. *EMBO J.* 9:4381–4390.

Lesage, F., E. Guillemare, M. Fink, F. Duprat, M. Lazdunski, G. Romey, and J. Barhanin. 1996a. A pH-sensitive yeast outward rectifier K$^+$ channel with 2 pore domains and novel gating properties. *J. Biol. Chem.* 271:4183–4187.

Lesage, F., E. Guillemare, M. Fink, F. Duprat, M. Lazdunski, G. Romey, and J. Barhanin. 1996b. TWIK-1, a ubiquitous human weakly inward rectifying K$^+$ channel with a novel structure. *EMBO J.* 15:1004–1011.

Miller, C. 1991. 1990: annus mirabilis of potassium channels. *Science.* 252:1092–1096.

Pascual, J. M., C.-C. Shieh, G. E. Kirsch, and A. M. Brown. 1995. Multiple residues specify external tetraethylammonium blockade in voltage-gated potassium channels. *Biophys. J.* 69:428–434.

Quick, M. W., and H. A. Lester. 1994. Methods for expression of excitability proteins in *Xenopus* oocytes. *In* Ion Channels of Excitable Cells. Academic Press, San Diego. 261–279.

Silverman, S. K. 1998. I. Conformational and Charge Effects on High-Spin Organic Polyradicals. II. Studies on the Chemical-Scale Origin of Ion Selectivity in Potassium Channels, Ph.D. thesis, California Institute of Technology, Pasadena, CA.

Silverman, S. K., P. Kofuji, D. A. Dougherty, N. Davidson, and H. A. Lester. 1996a. A regnerative link in the ionic fluxes through the weaver potassium channel underlines the pathophysiology of the mutation. *Proc. Natl. Acad. Sci. USA.* 1996:15429–15434.

Silverman, S. K., H. A. Lester, and D. A. Dougherty. 1996b. Subunit stoichiometry of a heteromultimeric G protein-coupled inward-rectifier K$^+$ channel. *J. Biol. Chem.* 271:30524–30528.

Tinker, A., Y. N. Jan, and L. Y. Jan. 1996. Regions responsible for the assemby of inwardly rectifying potassium channels. *Cell.* 87:857–868.

Tucker, S. J., M. Pessia, and J. P. Adelman. 1996. Muscarine-gated K$^+$ channel: subunit stoichiometry and structural domains essential for G protein stimulation. *Am. J. Physiol.* 271:H379–H385.

Velimirovic, B., E. Gordon, N. Lim, B. Navarro, and D. E. Clapham. 1996. The K$^+$ channel inward rectifier subunits form a channel similar to neuronal G protein-gated K$^+$ channel. *FEBS Lett.* 379:31–37.

Wei, A., T. Jegla, and L. Salkoff. 1996. Eight potassium channel families revealed by the *C. elegans* genome project. *Neuropharmacology.* 35:805–829.

Wei, A., C. Solaro, C. Lingle, and L. Salkoff. 1994. Calcium sensitivity of BK-type K$_{Ca}$ channels determined by a separable domain. *Neuron.* 13:671–681.

Wischmeyer, E., F. Doring, E. Wischmeyer, A. Spauschus, A. Thomzig, R. Veh, and A. Karschin. 1997. Subunit interactions in the assembly of neuronal Kir3.0 inwardly rectifying K$^+$ channels. *Mol. Cell. Neurosci.* 9:194–206.